

# Cardiolipin: characterization of distinct oxidized molecular species

Junhwan Kim,\* Paul E. Minkler,\*<sup>††</sup> Robert G. Salomon,<sup>†</sup> Vernon E. Anderson,<sup>§</sup> and Charles L. Hoppel<sup>1,\*††</sup>

Departments of Pharmacology,\* Chemistry,<sup>†</sup> Biochemistry,<sup>§</sup> and Medicine,\*\* and Center for Mitochondrial Diseases,<sup>††</sup> Case Western Reserve University, Cleveland, OH 44106

**Abstract** Cardiolipin (CL) is a phospholipid predominantly found in the mitochondrial inner membrane and is associated structurally with individual complexes of the electron transport chain (ETC). Because the ETC is the major mitochondrial reactive oxygen species (ROS)-generating site, the proximity to the ETC and bisallylic methylenes of the PUFA chains of CL make it a likely target of ROS in the mitochondrial inner membrane. Oxidized cellular CL products, uniquely derived from ROS-induced autoxidation, could serve as biomarkers for the presence of the ROS and could help in the understanding of the mechanism of oxidative stress. Because major CL species have four unsaturated acyl chains, whereas other phospholipids usually have only one in the *sn*-2 position, characterization of oxidized CL is highly challenging. In the current study, we exposed CL, under aerobic conditions, to singlet oxygen (<sup>1</sup>O<sub>2</sub>), the radical initiator 2,2'-azobis(2-methylpropionamide) dihydrochloride, or room air, and the oxidized CL species were characterized by HPLC-tandem mass spectrometry (MS/MS). Our reverse-phase ion-pair HPLC-MS/MS method can characterize the major and minor oxidized CL species by detecting distinctive fragment ions associated with specific oxidized species. The HPLC-MS/MS results show that monohydroperoxides and bis monohydroperoxides were generated under all three conditions. However, significant amounts of CL dihydroperoxides were produced only by <sup>1</sup>O<sub>2</sub>-mediated oxidation. These products were barely detectable from radical oxidation either in a liposome bilayer or in thin film. These observations are only possible due to the chromatographic separation of the different oxidized species.—Kim, J., P. E. Minkler, R. G. Salomon, V. E. Anderson, and C. L. Hoppel. **Cardiolipin: characterization of distinct oxidized molecular species.** *J. Lipid Res.* 2011. 52: 125–135.

**Supplementary key words** singlet oxygen • free radical • reactive oxygen species • reverse-phase ion pair • high-performance liquid chromatography-tandem mass spectrometry • lipid hydroperoxide

This work was supported by National Institutes of Health/National Institute on Aging Grant P01 AG-015885 and National Heart Lung and Blood Institute Grant P01 HL087018. Its contents are solely the responsibility of the authors and do not necessarily represent the official views of the National Institutes of Health.

Manuscript received 10 August 2010 and in revised form 16 September 2010.

Published, JLR Papers in Press, September 20, 2010

DOI 10.1194/jlr.M010520

The mitochondrial electron transport chain (ETC) is the major site of intracellular reactive oxygen species (ROS) generation (1, 2). The mitochondrially generated ROS are believed to contribute to the decrease in cellular function that accompanies aging (3) and numerous degenerative diseases (4–6). The most abundant ROS generated by mitochondria are superoxide (O<sub>2</sub><sup>•-</sup>) and hydrogen peroxide (H<sub>2</sub>O<sub>2</sub>).

Under normal conditions, O<sub>2</sub><sup>•-</sup> is disproportionated into O<sub>2</sub> and H<sub>2</sub>O<sub>2</sub> by superoxide dismutase and, in turn, H<sub>2</sub>O<sub>2</sub> is disproportionated into H<sub>2</sub>O and O<sub>2</sub> by catalase (7). Under some pathologic conditions, e.g., following ischemic-reperfusion injury, dysfunctional ETC complexes generate elevated levels of superoxide, overwhelming the antioxidant systems (8, 9). Although superoxide and H<sub>2</sub>O<sub>2</sub> are reported to directly cause oxidative damage in biological systems (10, 11), these ROS do not readily react with cardiolipin (CL). The most reactive ROS is the hydroxyl radical, which may be generated by the Fenton reaction, the Haber-Weiss reaction (12), and/or decomposition of peroxyxynitrite.

Recently, evidence has accumulated indicating that singlet oxygen (<sup>1</sup>O<sub>2</sub>) is generated in vivo and contributes to oxidative stress (13–16). Singlet oxygen is highly reactive and capable of oxidizing many biomolecules (17). Haber-Weiss decomposition of O<sub>2</sub><sup>•-</sup> and H<sub>2</sub>O<sub>2</sub> has been reported to generate both the hydroxyl radical and <sup>1</sup>O<sub>2</sub> (18). Singlet oxygen additionally may be generated by the reaction of H<sub>2</sub>O<sub>2</sub> or lipid hydroperoxides with the hypochlorite ion, whose generation by myeloperoxidase has become more fully appreciated (19–21).

However, it is a great challenge to prove the involvement of any specific ROS in biological systems under oxidative

Abbreviations: AAPH, 2,2'-azobis(2-methylpropionamide) dihydrochloride; CL, cardiolipin; DMPC, dimyristoylphosphatidyl choline; ETC, electron transport chain; MS, mass spectrometry; MS/MS, tandem mass spectrometry; ROS, reactive oxygen species.

<sup>2</sup>Present address of Vernon E. Anderson: Division of Pharmacology, Physiology and Biological Chemistry, National Institute of General Medical Sciences.

<sup>1</sup>To whom correspondence should be addressed.  
e-mail: charles.hoppel@case.edu

stress. Simply detecting a certain ROS does not necessarily prove its oxidative action, because the ROS detected may have been dispatched by antioxidants without causing any damage. Only oxidatively modified products of biomolecules that are unique to certain ROS will provide conclusive evidence of their role in oxidative stress.

CL is an unusual phospholipid localized to the mitochondrial inner membrane, where it interacts with proteins of the ETC. CL is required for inner membrane transporters such as the adenine nucleotide translocase (22). Because CL is enriched in PUFAs, primarily linoleic acid, and is located in close proximity to sites of ROS production in the mitochondrial ETC, it is a primary target for reaction with ROS.

Oxidation of CL causes dysfunction of mitochondrial ETC (23) and is proposed to contribute to the release of proapoptotic proteins, including cytochrome *c*, from the intermembrane space (24, 25). Because of their different chemical reactivities (12), the hydroxyl radical and  $^1\text{O}_2$  generate different oxidized products in their reactions with proteins (26, 27). In a similar manner, the different ROS could generate uniquely oxidized products of CL that provide important mechanistic information on oxidative stress. However, unlike other phospholipids, the multiple PUFAs of CL make its oxidized product characterization highly challenging.

Previously, we exposed liposomal CL and mitochondria to  $^1\text{O}_2$  generated by the photosensitizer Pc 4 and light, and the oxidized products were analyzed by direct infusion ESI-tandem mass spectrometry (MS/MS) (28). This photosensitizer generates a relatively pure source of  $^1\text{O}_2$  (29), and CL was suggested as an initial target (30, 31). In the liposome oxidations, we identified two major products with mass increments of +32 and +64 whose MS/MS spectra suggest the existence of at least two isomers for each species. In mitochondria illuminated in the presence of Pc 4, only the +32 species were identified (28).

In the current study, we exposed CL to  $^1\text{O}_2$ , the free-radical initiator 2,2'-azobis(2-methylpropionamide) dihydrochloride (AAPH), or room air, and characterized the oxidized CL by reverse-phase ion pair HPLC-MS/MS. Under the reaction conditions examined, all of these oxidations produced monohydroperoxides and bis monohydroperoxides (CLs containing two monohydroperoxyl chains). Furthermore, only  $^1\text{O}_2$  treatment led to the formation of significant amounts of dihydroperoxides of CL (CLs containing one dihydroperoxyl chain). The HPLC-MS/MS procedure that we developed can separate the three species and partially resolve the isobaric structural isomers in each species, which give rise to different fragmentation patterns detected by MS/MS.

## MATERIALS AND METHODS

CL and AAPH were purchased from Sigma-Aldrich (St. Louis, MO), dimyristoylphosphatidyl choline (DMPC) from Avanti

Polar Lipids (Alabaster, AL), and Whatman TLC plates from Fisher Scientific (Pittsburgh, PA). Pc 4 was a generous gift of Dr. Malcolm E. Kenney (Case Western Reserve University, Cleveland, OH). Millipore water (18 M $\Omega$ ) was used throughout.

### Reverse-phase ion pair HPLC-MS/MS

The reverse-phase ion pair HPLC-MS/MS system consisted of an HP1100 series quaternary pump with an on-line degasser, autosampler, and column heater (Agilent Technologies, Wilmington, DE). A Symmetry<sup>®</sup> C18 5  $\mu\text{m}$ , 150  $\times$  3.9 mm analytical column (Waters Corporation, Milford MA) was used. Gradient elution used two eluents: eluent A (450 ml acetonitrile, 50 ml water, 2.5 ml triethylamine, and 2.5 ml glacial acetic acid) and eluent B (450 ml 2-propanol, 50 ml water, 2.5 ml triethylamine, and 2.5 ml glacial acetic acid). The combination of triethylamine and acetic acid in both eluents dynamically forms ion pairs with the negatively charged phosphates in the CL molecule, resulting in increased chromatographic retention and greatly improved chromatographic resolution. Initially, 50%A-50%B was eluted at a flow rate of 400  $\mu\text{l}/\text{min}$ , and this was maintained for 5 min following the injection. Then, a linear gradient to 80% B over 10 min, followed by a gradient to 100% B over 15 min, and finally a hold at 100% B for 10 min completed the chromatographic run. A 3200 Q TRAP<sup>®</sup> hybrid triple quadrupole/linear ion trap mass spectrometer, with a Turbo V<sup>TM</sup> ion source (Applied Biosystems/MDS SCIEX; Concord, Ontario, Canada) was used. The source was operated in the Turbo IonSpray negative-ion configuration. The instrument's linear ion trap mode was employed with an information-dependent acquisition method, which included a survey scan in the enhanced mass spectrometry (MS) mode followed by an enhanced product ion scan on the most intense ion in the enhanced MS scan. The enhanced MS scan was performed at a rate of 250 Da/s with a spectral range of 1,400–1,600 Da, and the enhanced product ion scan was performed at a rate of 1,000 Da/s with a spectral range of 100–900 Da (32).

### Liposome preparation

Vesicles containing DMPC and CL (total 2 mM containing 20% CL) were prepared with a Mini-Extruder from Avanti Polar Lipids, Inc. (Whatman<sup>®</sup> membrane diameter  $\cong$  100 nm). Typically, an aliquot of lipid solution in absolute ethanol was evaporated to form a thin film of lipid. PBS (pH 7.4, 0.1 M  $\text{NaH}_2\text{PO}_4$  and  $\text{K}_2\text{HPO}_4$ , and 0.15 M NaCl) was added to hydrate the film, and the lipid mixture was extruded at 45°C. Incorporation of Pc 4 was achieved by adding a solution of Pc 4 in THF/EtOH (1:1) and incubating the liposome-Pc 4 complex at 45°C for 30 min with stirring. All procedures were performed while minimizing the exposure of the lipids to air or light.

### Oxidation of CL

For  $^1\text{O}_2$ -mediated oxidation, liposomes containing the photosensitizer Pc 4 were exposed to 100 mW/cm<sup>2</sup> red light produced by a light-emitting diode array (EFOS; Mississauga, Ontario, Canada;  $\lambda_{\text{max}}$  670–675 nm) at room temperature for 20 min. Radical oxidation of CL was initiated by adding 60 mM AAPH to the liposomes and incubating for 5 min at 37°C. Air oxidation of CL was performed by exposing a thin film of CL in a test tube to air for 24 h. Lipids were extracted from 0.5 ml of the DMPC+CL liposome solution using 1.5 ml of  $\text{CHCl}_3$ -MeOH (2:1). The extract was dried under a stream of  $\text{N}_2$  and redissolved in 20  $\mu\text{l}$   $\text{CHCl}_3$ . The solution was dispensed on silica gel TLC plates, developed with  $\text{CHCl}_3$ -MeOH-acetic acid- $\text{H}_2\text{O}$  (3:0.52:0.36:0.12) (33) and visualized by  $\text{I}_2$ . The CL spot was scraped into a 0.6 ml microcentrifuge tube and extracted using 100  $\mu\text{l}$   $\text{CHCl}_3$ -MeOH (1:1). The conditions for each oxidation were adjusted following prelimi-

nary experiments to give similar relative content of oxidized CL species (~30%).

## RESULTS

### Characterizing control CL by reverse-phase ion pair HPLC-MS/MS

CL is a phospholipid with a central glycerol connected by phosphodiester linkages at C1 and C3 to two diacylglycerol phosphatidic acid moieties. The fragmentation of the singly charged tetralinoleoyl CL negative ion  $[M - H]^-$  results in fragments observed in the  $m/z$  region between 200 and 900 by MS/MS (Fig. 1). These peaks and corresponding fragments have been reported previously (34, 35). The different relative intensities of the peaks, which are advantageous to our study, are due to the different configurations of the ion traps used (36). The three most intense peaks correspond to free linoleate ( $m/z$  279), monoacylglycerol phosphatidate ( $m/z$  415), and diacylglycerol phosphatidate ( $m/z$  695). Assignments of fragmented oxidized CL products were accomplished by examining their mass increments or losses based on these three peaks. Importantly, there are no fragment ions observed from cleavage of the unoxidized linoleic acyl chains from each moiety.

### $^1O_2$ -induced CL oxidation analyzed by reverse-phase ion pair HPLC-MS/MS

CL in liposomes was exposed to  $^1O_2$ . The chromatogram of CL oxidized by  $^1O_2$  shows unmodified CLs eluting at >26 min and oxidation products eluting at 22–23, 20–21, and 16–17 min (Fig. 2A). Because oxidation decreases the hydrophobicity of the side chain, the CL species suffering the greater oxidation elute earlier.

The MS and MS/MS spectra of the analytes eluting around 22–23 min are shown in Fig. 2B. These are the least-oxidized products. The most-abundant ions are singly charged, with  $m/z$  1479, 32 Da greater than the  $[M - H]^-$  of tetralinoleoyl CL. To discriminate between hydroperoxide, endoperoxide, and dihydroxide modifications, the oxidized CL was treated with a reducing agent (sodium borohydride). This reduction resulted in the elimination of the peak at  $m/z$  1479, with a concomitant increase in the peak at  $m/z$  1463 (–16 from 1479), when analyzed by direct infusion (data not shown). This mass loss is consistent with the reduction of hydroperoxides to hydroxides, which supports the assignment of this CL species to isomers with one hydroperoxyl group. Careful examination of the same chromatographic peak results in the detection of very minor peaks, with  $m/z$  1463 in this region attributed to isomeric CLs bearing a single

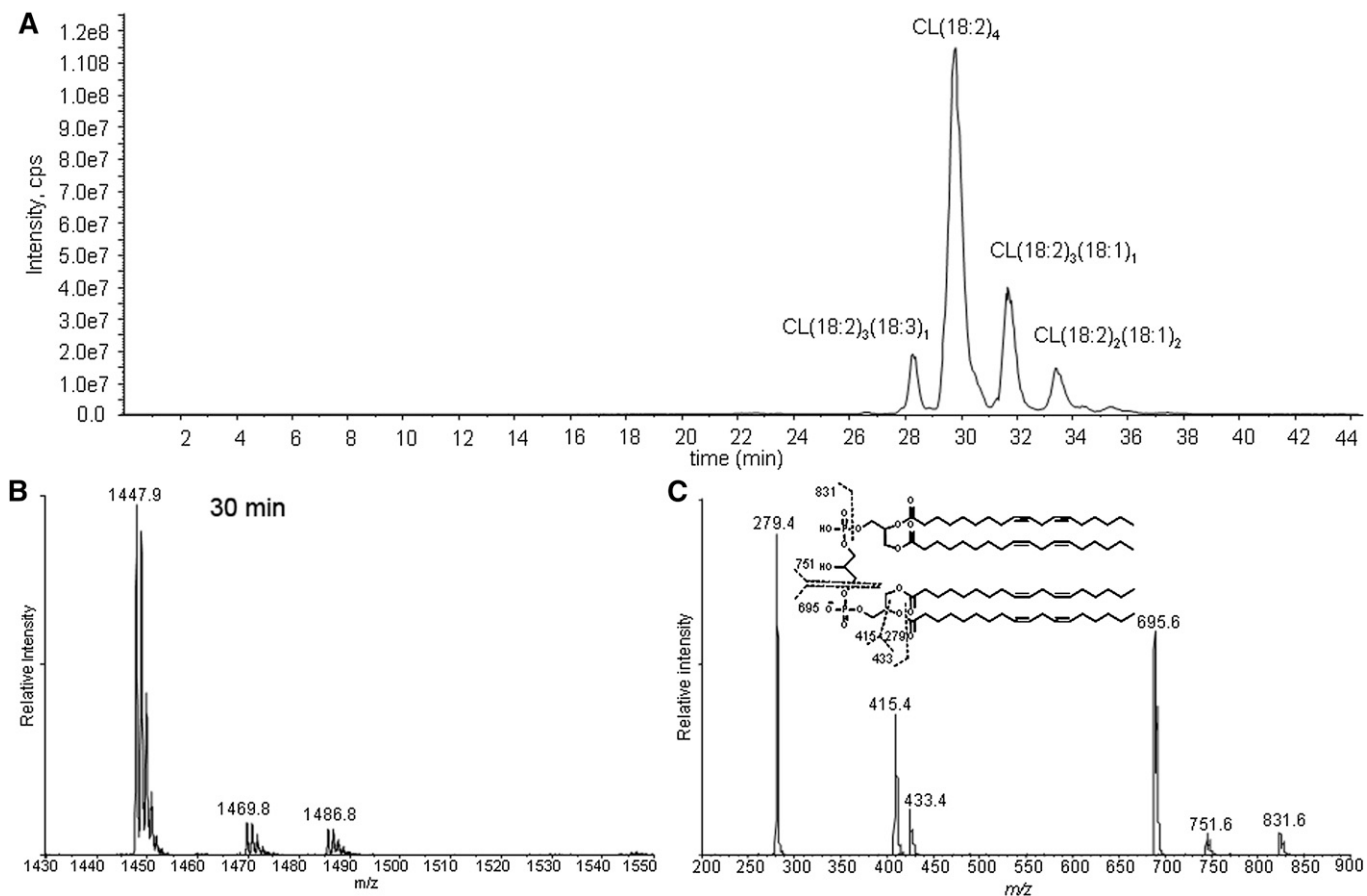


**Fig. 1.** Total ion chromatogram of control cardiolin (CL) (A), mass spectrometry (MS) spectrum (B), and tandem mass spectrometry (MS/MS) spectrum (C) of the chromatographic peak at 30 min. The major species in the peak at 30 min has an  $m/z$  of 1447, consistent with tetralinoleoyl CL. The MS/MS spectrum shows the characteristic fragment ions  $m/z$  831, 751, 695, 433, 415, and 279. Proposed fragmentation of tetralinoleoyl CL is shown in the inset of C.

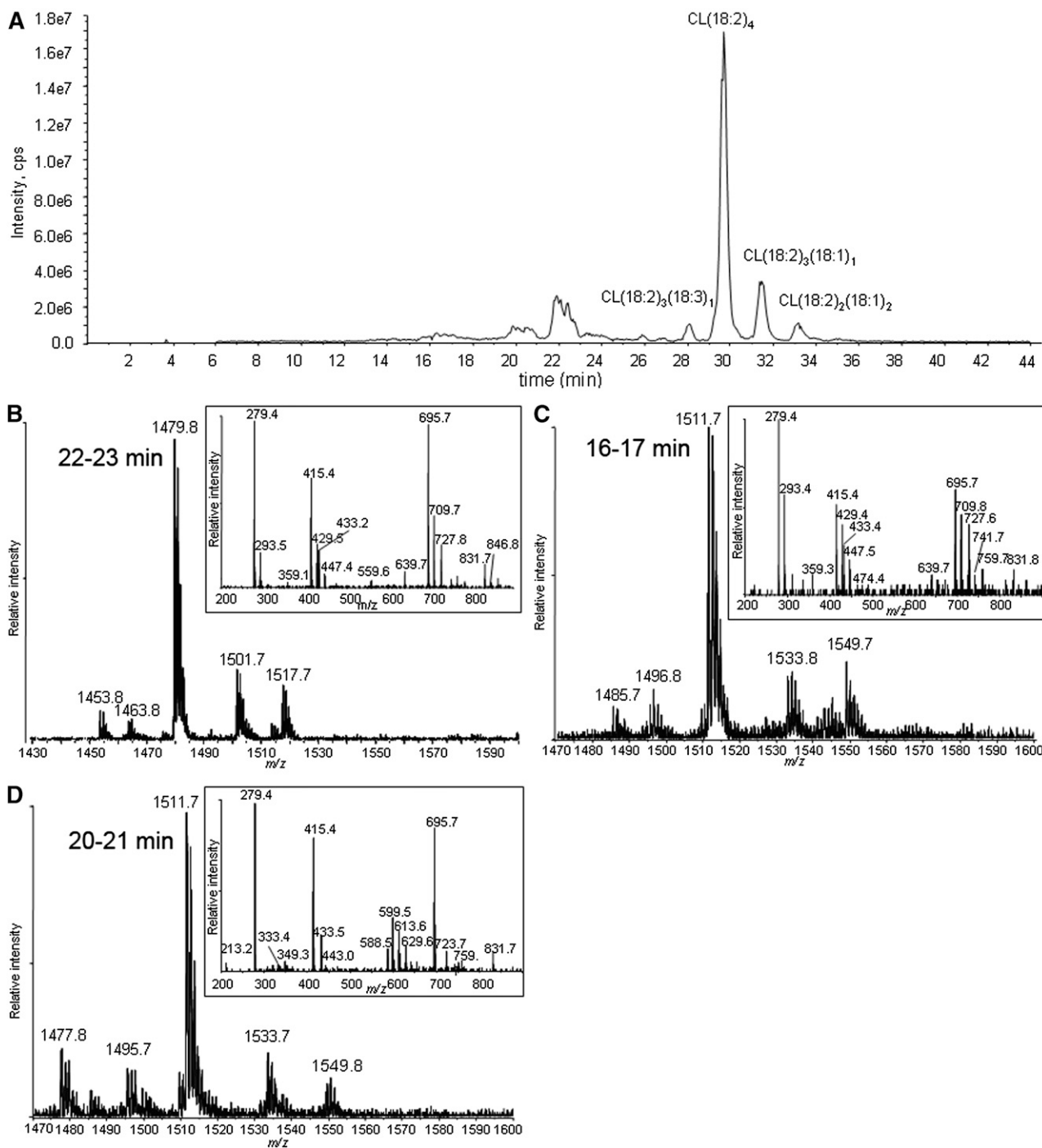


**Fig. 2.** Total ion chromatogram of CL oxidized by Pc 4-mediated  $^1\text{O}_2$  (A), and MS and MS/MS spectra of the chromatographic peaks at 22–23 min (B), 16–17 min (C), and 20–21 min (D). The major species in the peak at 22 min have *m/z* 1479 (A), corresponding to monohydroperoxides, and the inset shows all the characteristic fragment ions with *m/z* 727, 709, 447, 429, and 293 generated from monohydroperoxides. MS spectra of the chromatographic peaks at 16–17 (C) and 20–21 (D) min show that the major species in these regions have *m/z* 1511, but fragment ions observed in MS/MS spectra suggest the species are bis monohydroperoxides and dihydroperoxides, respectively.

hydroxyl group, showing that hydroxides coelute with hydroperoxides.

Also at 22–23 min, the peaks in the mass spectrum with *m/z* 1501 and 1517 are attributed to  $[\text{M} + 2\text{O} - 2\text{H}^+ + \text{Na}^+]^-$  and  $[\text{M} + 2\text{O} - 2\text{H}^+ + \text{K}^+]^-$ , respectively. These precursor ions share the characteristic fragment ions of monohydroperoxides, as shown in a typical MS/MS in the inset of

Fig. 2B. The observed fragment ions at nominal *m/z* 695 and 727 correspond to the unmodified and monohydroperoxyl diacylglycerol phosphatidic acid moieties from the  $[\text{M} + 2\text{O} - \text{H}^+]^-$ . The *m/z* 709 ion derives from the dehydration typically observed with lipid hydroperoxides. That this dehydration occurs with the monohydroperoxides and not the underivatized CL and phosphatidic acid

supports the conclusion that the loss of water comes from cleavage of the O-O peroxide bond. In the free acyl region (linoleic acid  $m/z$  279), the presence of  $m/z$  293 and barely detectable  $m/z$  311 ions indicate that this dehydration took place to a greater extent during the fragmentation that generates the acyl chain anion. The monoacylglycerol phosphatidic acid fragment ions at  $m/z$  415, 429, and 447 reflect the presence of unmodified and hydroperoxyl fragment ions. The ready loss of water from fragment ions containing hydroperoxides has been previously noted (37, 38). All of the fragment ions are consistent with the assignment of the  $m/z$  1479 precursor as monohydroperoxide isomers of CL.

The MS/MS spectrum also shows fragment ions derived from cleavage of hydroperoxyl-modified linoleic acyl chains. These acyl chain fragmentations can be detected most readily as neutral losses from the hydroperoxyl-modified diacylglycerol phosphatidic acid fragment. The peaks at  $m/z$  639 (mass loss of 88 Da from 727) and 559 (mass loss of 168 Da from 727) are interpreted as arising from cleavage on the saturated side of the conjugated dienyl-hydroperoxide, as shown in Fig. 3. These mass losses are consistent with the presence of 13- and 9-hydroperoxides, respectively, as previously described (39). The MS/MS spectra reveal that the peak at  $m/z$  639 dominates at earlier retention times (Fig. 3A), whereas the peak at  $m/z$  559 is more intense at later times (Fig. 3B), indicating that the 13-hydroperoxides, which contain a shorter "alkyl tail" elute earlier than the 9-hydroperoxides.

As shown in Fig. 2C, D, the major species in the chromatographic peaks at 16–17 and 20–21 min are isobaric species with  $m/z$  1511 interpreted as a  $[M + 4O - H]^+$  ion. Reduction of these hydroperoxides with sodium borohydride results in a loss of 32 Da, suggesting that the  $m/z$  1511 ion (Fig. 2C, D) corresponds to incorporation of two hydroperoxyl groups in CL (1447). These isobaric species are attributed to CL, in which the hydroperoxyl moieties are on different acyl chains (bis monohydroperoxides) or the hydroperoxyls are on the same linoleoyl chain (dihydroperoxides). The structures of the bis monohydroperoxides and dihydroperoxides were further characterized by MS/MS.

Two major isomeric bis monohydroperoxide species can be further differentiated by MS/MS; species with one hydroperoxyl group on each diacylglycerol phosphatidic acid moiety or both hydroperoxyl groups on one diacylglycerol phosphatidic acid moiety. The proposed structures of the fragment ions from these two species observed by MS/MS are shown in Fig. 4. The observed characteristic fragment ions for the former are  $m/z$  727 and 709 (Fig. 5A), and for the latter  $m/z$  759, 723, and 695 (Fig. 5B). However, when the diacylglycerol phosphatidic acid moieties further lose one acyl chain, both isomeric bis monohydroperoxide species will generate the same fragment ions as observed at  $m/z$  447, 429, 415, 311, 293, and 279. It was found that the intensities of ions at  $m/z$  727 and 709 are higher than those with  $m/z$  695 and 759 at the earlier retention time (Fig. 5), suggesting that CL species with hydroperoxyl groups on each diacylglycerol phosphatidic acid moiety have shorter retention times than the species with both hydroperoxyl groups on one diacylglycerol phosphatidic acid moiety. The observation of a peak with  $m/z$  359 (mass loss of 88 from 447) suggests the existence of the species with a hydroperoxyl group in the 13 position.

Close examination of the MS spectra of the eluting chromatographic peaks revealed that both  $m/z$  1511 peaks in Fig. 2C, D coeluted with barely detectable  $m/z$  1495 peaks, whose MS/MS spectrum suggests modification of the parent CL by one hydroxyl and one hydroperoxyl group. A CL species with  $m/z$  1477 found in Fig. 2D, predicted to be derived from hydroperoxyl CL(18:2)<sub>3</sub>(18:3)<sub>1</sub>, also eluted in the region of the chromatogram containing these dihydroperoxides, indicating that the additional unsaturation had an effect on retention time similar to that of the addition of the second hydroperoxyl group.

The key feature of the MS/MS spectrum of the chromatographic peak at 20–21 min in Fig. 2D, with the precursor ion of  $m/z$  1511, is the lack of any characteristic fragment ions derived from monohydroperoxyl acyl chains, namely  $m/z$  727, 709, 447, 429, 311, or 293. The  $m/z$  723 ion (inset) resulted from the loss of two water

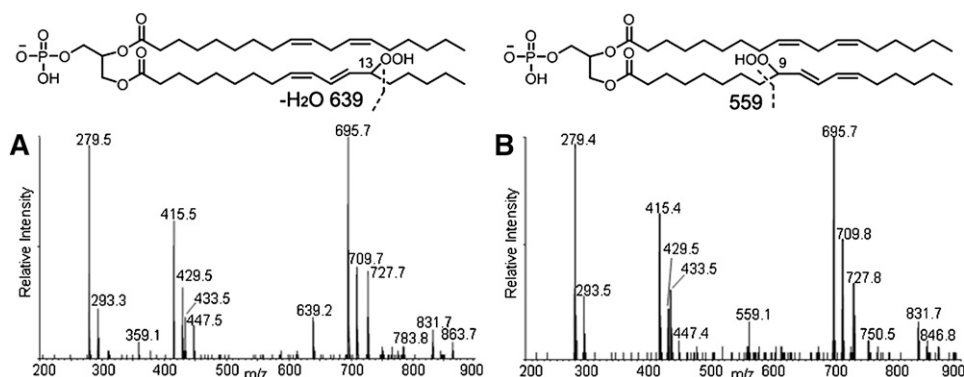


**Fig. 3.** MS/MS spectra and structures of corresponding hydroperoxides of the first 45 s (A) and last 45 s (B) of the chromatographic peak at 22–23 min. The characteristic fragment ion of 13-monohydroperoxides,  $m/z$  639, was only found in A and of 9-hydroperoxides,  $m/z$  559, only in B, suggesting that the former elutes earlier than the latter.

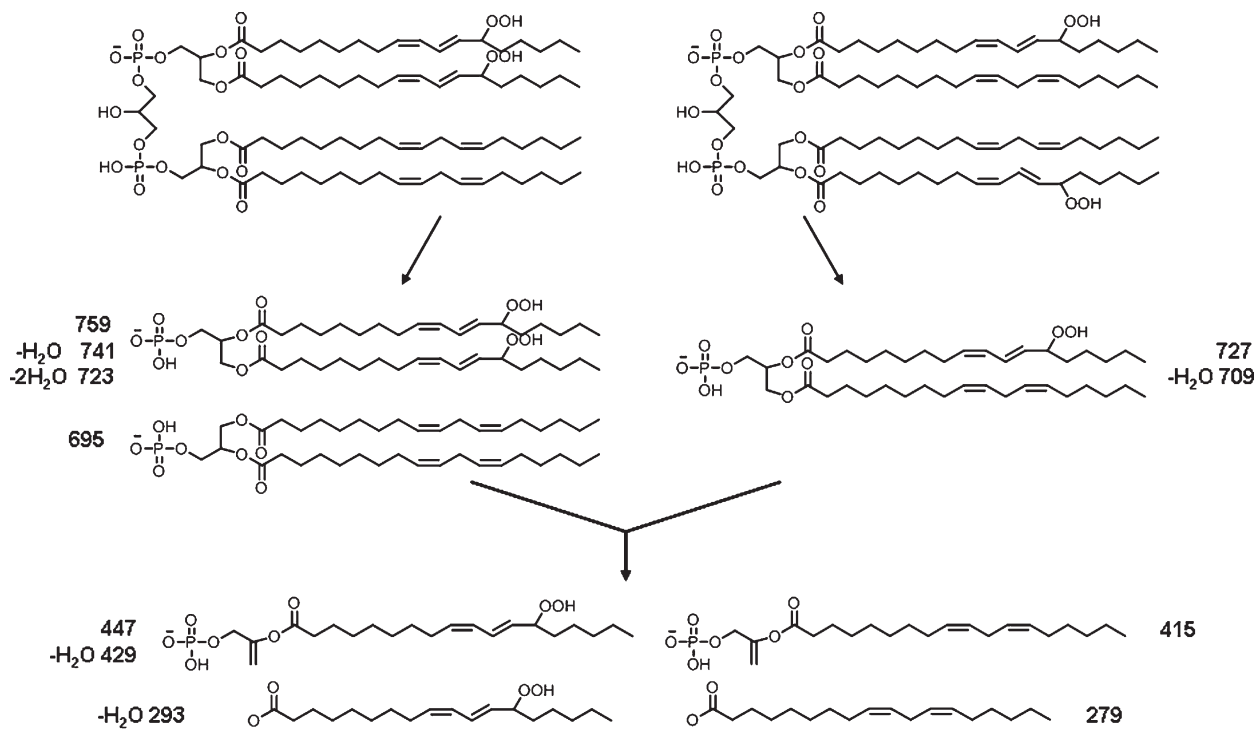


**Fig. 4.** Proposed fragment ions from two major isomeric bis monohydroperoxides showing species with both hydroperoxyl groups on one glycerol moiety and one hydroperoxyl group on each glycerol moiety.

molecules from dihydroperoxyl diacylglycerol phosphatidic acid, and fragment ions at  $m/z$  588, 599, 613, and 629 derived from cleavage of a dihydroperoxyl linoleic acyl chain strongly support the assigned dihydroperoxide structure for the modified CLs eluting as the major species at this time (Fig. 2D). Although the peaks at  $m/z$  599 and 613 may be generated from fragmentation of 10,12-dihydroperoxides and the peak at  $m/z$  588 from 9,12-dihydroperoxides (Fig. 6), these assignments, without precedent MS/MS data, remain tentative until confirmed by synthesis of authentic material or other characterizations. We speculate that the presence of the easily fragmented acyl chain containing two hydroperoxyl groups may be responsible for the low intensity for peaks of the corresponding diacylglycerol phosphatidic acid, monoacylglycerol phosphatidic acid, and free linoleate.

#### Free radical-initiated oxidation of CL

Free radical-initiated oxidation of CL gives +32 and +64 as major oxidized products observed by MS analysis. Aerobic radical-initiated oxidation generated significant amounts of monohydroperoxides and bis monohydroperoxides but no observable dihydroperoxides, as shown in the HPLC-MS total ion chromatogram of Fig. 7A.

The MS spectrum of the peak at 22–23 min showed two major species, with  $m/z$  1479 and 1463 (Fig. 7B), suggesting the presence of significant amounts of hydroperoxides as well as hydroxides. The formation of hydroxides was found to occur during the preparation of vesicles, and the relative intensity of the peak decreased as the peaks of hydroperoxides increased by the radical-induced oxidation. Addition of a chelating agent, diethylene triamine pentaacetic acid, did not reduce the intensity of the peak at  $m/z$

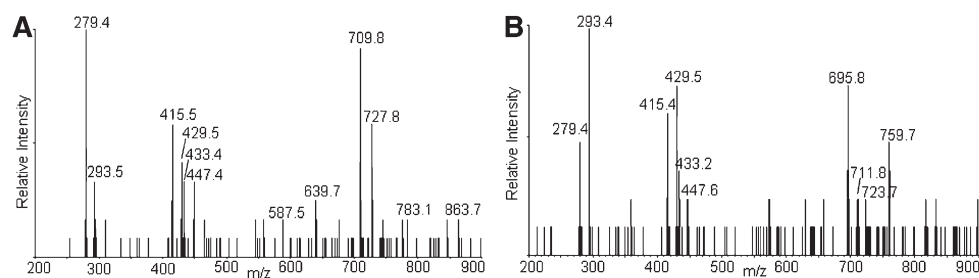


**Fig. 5.** MS/MS spectrum of first 45 s (A) and last 45 s (B) of chromatogram peak at 16–17 min. The characteristic fragment ions from species with one hydroperoxyl group on each phosphatidic acid moiety,  $m/z$  709 and 727, were only found at an earlier retention time, and fragment ions from species with two hydroperoxyl groups on one phosphatidic acid moiety,  $m/z$  759, 723, and 695, at a later retention time, suggesting that the former eluted earlier than the latter.

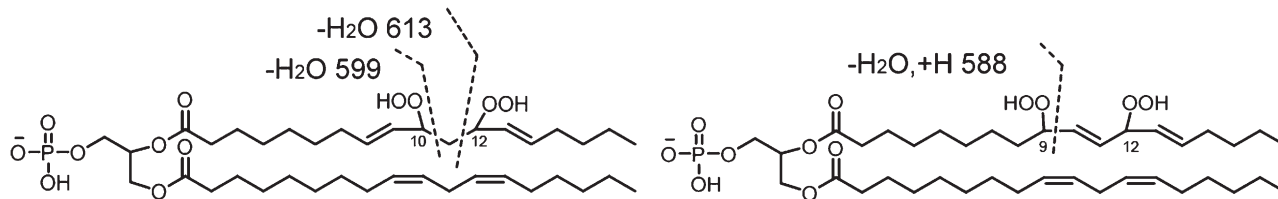


**Fig. 6.** Proposed structures of 10, 12-dihydroperoxyl phosphatidyl glycerol and 9, 12-dihydroperoxyl phosphatidyl glycerol moieties with fragment ions derived from cleavages on the dihydroperoxyl acyl chain.

1463 or affect oxidized products of CL (data not shown). The MS/MS spectrum of the same chromatographic peak shows the characteristic fragment ions from monohydroperoxides also found in  $^1\text{O}_2$ -generated monohydroperoxides. The ions derived from the cleavage of the linoleic acyl chain (ions at  $m/z$  640, 359, and 559) support the assertion that the major species are 13- and 9-hydroperoxides.

The MS spectrum of the chromatographic peak at 16–17 min also contains hydroxyl species, although bis monohydroperoxides still constitute the most prominent ions (Fig. 7C). The peak with  $m/z$  1479 suggests that bis monohydroxides coeluted at this retention time. MS/MS spectra of the same chromatographic peak contain all of the characteristic fragment ions of bis monohydroperoxides, ions with  $m/z$  728, 710, 447,

429, and 293, and bis monohydroxides, observable ions with  $m/z$  712 and 431. The positions of the hydroperoxide modifications are suggested to be at C13 and C9 by the peaks with  $m/z$  640, 359, and 559. The peaks at  $m/z$  728 and 760 suggest that free-radical oxidation also can generate both species with both hydroperoxyl groups on one glycerol moiety and one hydroperoxyl group on each glycerol moiety, as shown in Fig. 4.

There is a very small chromatographic peak at 20 min with an  $m/z$  1477, predicted to be hydroperoxyl CL(18:2)<sub>3</sub>(18:3)<sub>1</sub>. Fragment ions observed in the MS/MS spectrum of this peak are consistent with this oxidized CL species, as noted earlier for Fig. 2D. The accumulated MS spectrum of this region of the chromatogram also revealed a barely detectable peak at  $m/z$  1511, whose molecular weight corresponds to dihydroperoxides.

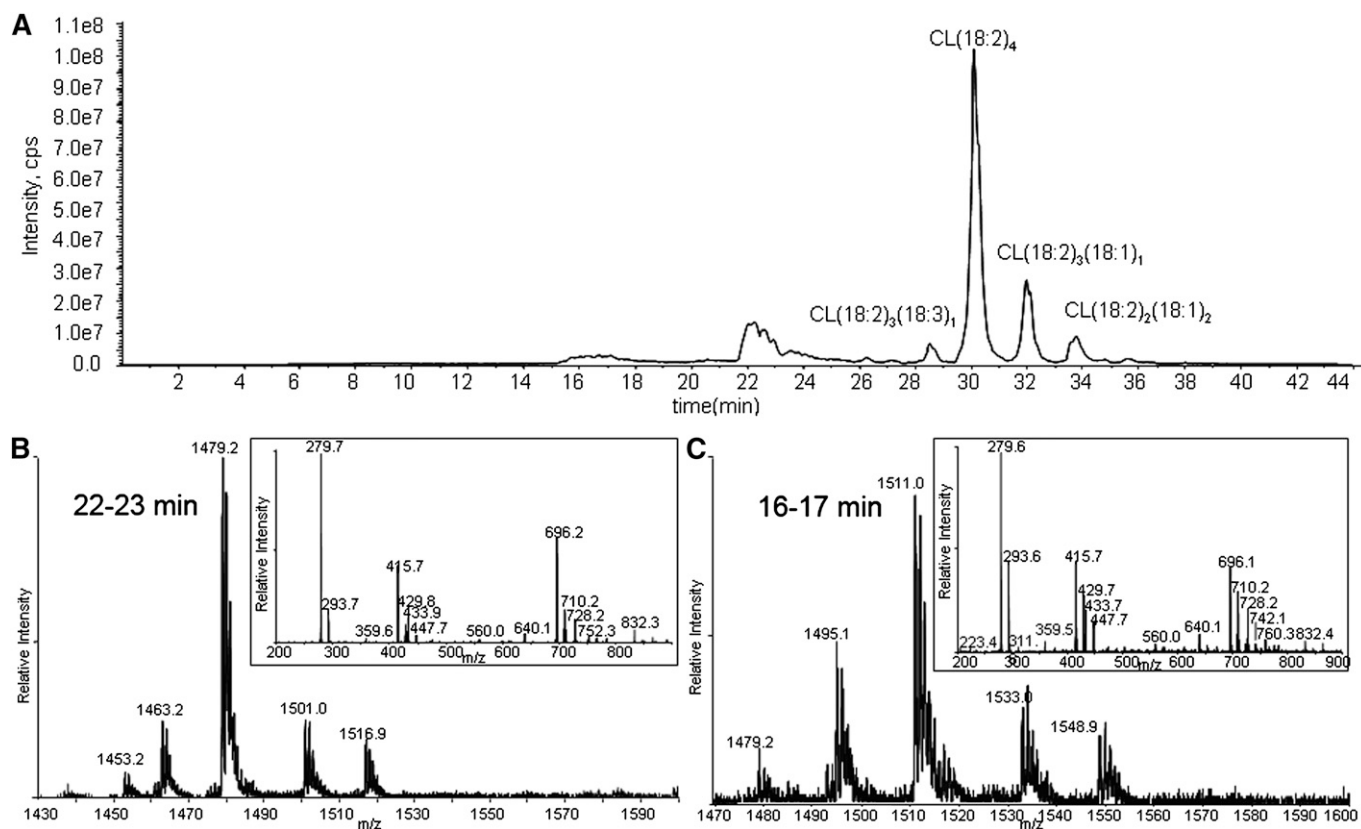


**Fig. 7.** Total ion chromatogram of CL oxidized by 2,2'-azobis(2-methylpropanamide) dihydrochloride-generated free radical (A), and MS and MS/MS spectra of peaks at 22–23 min (B) and 16–17 min (C). MS and MS/MS spectra of the peak at 22–23 min show that the major species present in this region have  $m/z$  1479 (B), corresponding to CL with either one hydroperoxyl group or with one hydroxyl group. Two major species found in the peak at 16–17 min of the chromatogram by MS and MS/MS spectra have  $m/z$  1511 and 1495 (C), corresponding to CL with two hydroperoxyl groups and with one hydroperoxyl and one hydroxyl group, respectively.

With extended reaction time (20 min), the intensity of the peak at  $m/z$  1511 increased with concomitant increases in the intensities of the other oxidized species of CL. However the intensity of the peak at  $m/z$  1511 is still negligible and the signal-to-noise ratio of the peak is less than 3.

### CL oxidation by room air

Exposing a dried film of CL to air for 24 h also produced a similar amount of oxidized species through autoxidation. The major products observed by HPLC-MS/MS were monohydroperoxide and bis monohydroperoxide species, without any significant amount of hydroxide species (Fig. 8). Similar MS/MS spectra of both chromatographic peaks at 18–19 and 24–25 min suggest that air oxidation generates the same monohydroperoxide and dihydroperoxide products as the other two ROS, with no significant dihydroperoxides.

## DISCUSSION

### Reverse-phase ion pair HPLC-MS/MS analysis of CL

The chromatograms of oxidized CL clearly showed that only  $^1\text{O}_2$  generated significant amounts of all three major species of oxidized products, whereas radical reaction generated only monohydroperoxides and bis monohydroperoxides (Scheme 1). The chromatographic separation of the three species of oxidized products was necessary to

make this determination, and the inclusion of a chromatographic component in our methodology is fundamental to our approach. The general observation has been made that analysis by MS alone can yield incorrect results, owing to the presence of unknown products generating unanticipated fragment ions, resulting in false-positive results (40). In our specific case, although the isobaric isomers of oxidized CL are indistinguishable by mass, these same compounds can be chromatographically resolved and structurally characterized, as we have demonstrated (Figs. 2, 7). Although the observed corresponding characteristic fragment ions and consistent chromatographic retention times of each species strongly support the structures as proposed, further characterizations of physically separated individual oxidized products and analysis of synthesized authentic standards will be necessary to differentiate the detailed structures and quantify the relative yields of the many species suggested by the chromatographic results.

### Responsible ROS: radical versus $^1\text{O}_2$

Superoxide and  $\text{H}_2\text{O}_2$  are the primary ROS generated by the mitochondrial ETC. Although certain oxidative damage caused by superoxide and  $\text{H}_2\text{O}_2$  has been reported (10, 11), these ROS do not readily react with biomolecules, especially CL. Rather, the hydroxyl radical derived from superoxide and  $\text{H}_2\text{O}_2$  by a Fenton-type or Haber-Weiss reaction is considered to be the main ROS responsible for most cellular oxidative damage (12). The hydroxyl radical is considered the most reactive ROS found in biological

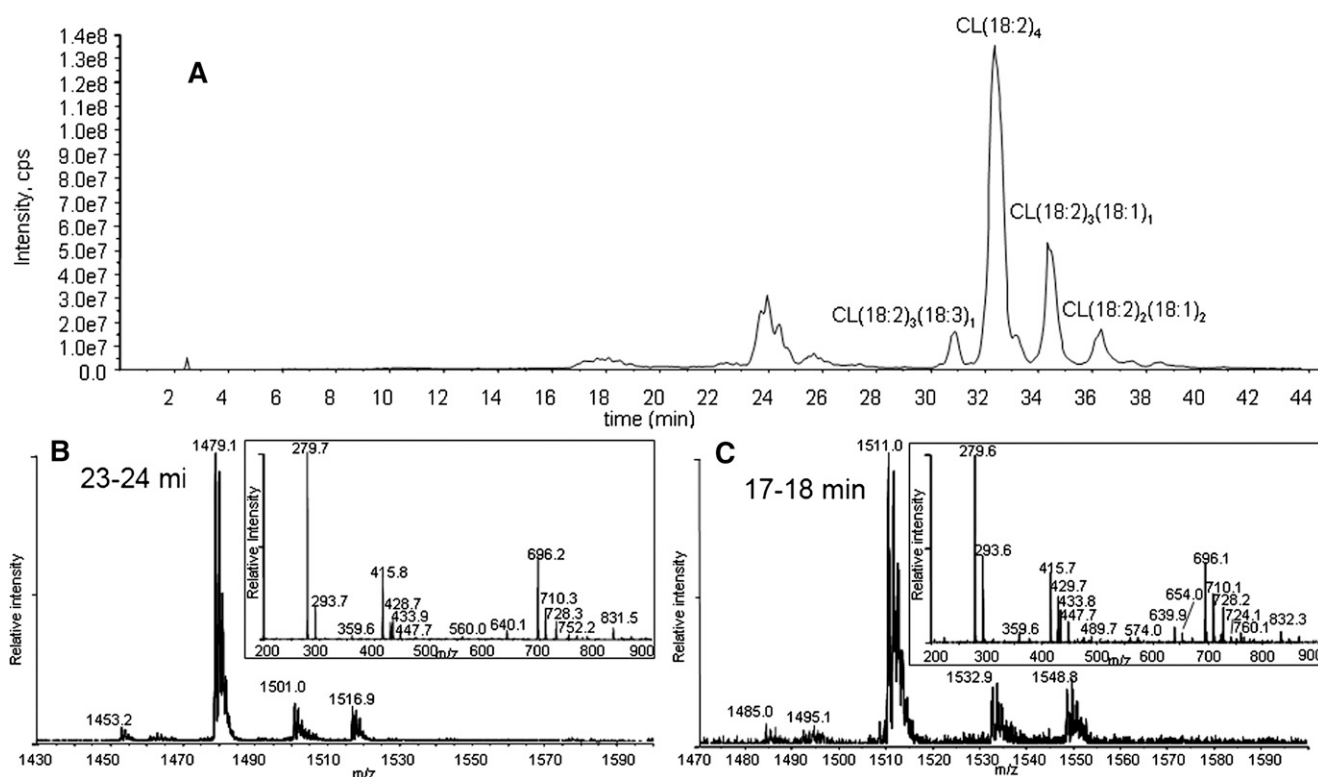
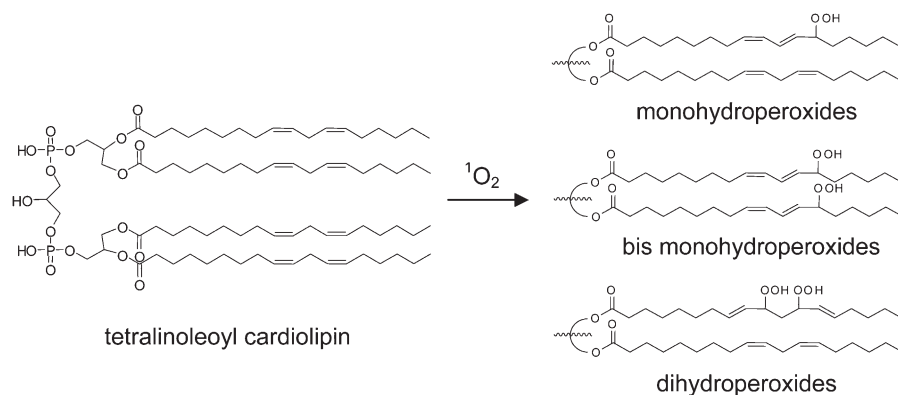


**Fig. 8.** Total ion chromatogram of CL oxidized by room air (A), and MS and MS/MS spectra of peaks at 23–24 min (B) and at 17–18 min (C). The major species in the chromatogram peak at 23–24 min have  $m/z$  1479 (B) and at 17–18 min  $m/z$  1511 (C), corresponding to bis monohydroperoxides and monohydroperoxides, respectively. The retention times of all species were delayed by  $\sim 1$  min compared with the chromatographic peaks of CL oxidized by  $^1\text{O}_2$  due to a different eluent batch.





**Scheme 1.** Representative structures of oxidized CL species consistent with HPLC-MS/MS spectral data.  $^1\text{O}_2$ -mediated oxidation generated all three types of structures, whereas the radical oxidation generated only monohydroperoxides and bis monohydroperoxides as major products.

systems. Nonetheless, there has been increasing evidence suggesting a role for  $^1\text{O}_2$  in various forms of oxidative stress, e.g., ischemia-reperfusion (13, 41, 42), aging-associated mitochondrial DNA lesions (43), and UV-A-mediated skin damage (15, 43). In spite of the fact that several mechanisms have been proposed for generation of  $^1\text{O}_2$  in biological systems and that the reactivity of  $^1\text{O}_2$  toward biomolecules has been demonstrated by *in vitro* studies, there is still a lack of direct evidence for involvement of  $^1\text{O}_2$  in any of the forms of oxidative stress.

In biological systems, simply detecting a particular ROS may not be sufficient to prove its role in oxidative stress, because the ROS detected may be dispatched by antioxidants or converted into more-reactive ROS (or reactive nitrogen species), depending on the microenvironment around the ROS generated. The amount of ROS does not necessarily correlate with the degree of oxidative damage (44). Therefore, oxidized products of biomolecules uniquely derived from a particular ROS may provide conclusive evidence to identify the responsible ROS.

Dihydroperoxides, generated in this unambiguous model system using  $^1\text{O}_2$ , may be the chemotype of  $^1\text{O}_2$ . The presence of dihydroperoxides is convincingly demonstrated from these data only under  $^1\text{O}_2$ -mediated oxidation, not under radical oxidation. Because the extent of oxidized CL found both *in vivo* and *in vitro* experiments is moderate (45–48), our approach, in which  $\sim 30\%$  of CL was oxidized, is sufficient to identify these products.

However, we cannot rule out the possibility that radical-mediated oxidation could generate significant amounts of dihydroperoxides. The conditions used for radical oxidation, e.g., concentration of AAPH, reaction time, or temperature, may not be optimal for dihydroperoxides to accumulate, or the steady state favors only low concentrations of dihydroperoxides in the presence of a continuous radical flux. Additional experimental examination of the generation and/or decomposition of individual dihydroperoxide species under various conditions will be required to resolve these questions. These investigations also may lead to the detection of specific dihydroperoxide isomers, which will serve as unequivocal biomarkers for  $^1\text{O}_2$ .

An additional intriguing result of these studies is the absence of any chain-cleaved CL oxidation products. *In vivo* aldehydes, e.g., 4-hydroxynonenal and other thiobarbituric acid-reactive substances derived from linoleic acid oxidation, have been used as monitors of oxidative stress. These products, readily generated from linoleic acid in the presence of a one-electron reductant, routinely reduced metal ions like Fe(II) (49, 50). The results of our studies suggest that production of aldehyde byproducts requires, in addition to oxygen radicals and/or singlet oxygen, a source of electrons to reduce the initial hydroperoxides.


#### Reaction mechanism for dihydroperoxides

The result that  $^1\text{O}_2$  generates significant amounts of dihydroperoxides, whereas free-radical oxidation does not, may be attributable to different reaction mechanisms of these two ROS. One chemical rationale for this differential reactivity comes from considering the structure of the monohydroperoxides. The initial step of oxidation by free radicals with a linoleic acyl chain is abstraction of hydrogen from the bis allylic carbon. The resulting dienoyl radical reacts more readily at the 9 or 13 position, resulting in 9- or 13-monohydroperoxylys, which subsequently abstract an H-atom from a donor. The stability of the conjugated diene-hydroperoxide will hinder the further hydrogen abstraction from this acyl group (51, 52). Rather, free radicals will abstract a hydrogen from a more-reactive bisallylic methylene of another acyl chain. This phenomenon will be more significant in biological systems in which the amount of free radical is limited.

This contrasts with the behavior of singlet oxygen-mediated oxidation. Because singlet oxygen reacts readily with conjugated dienes, the rate constant for reaction with 2,4-hexadiene is faster than that for reaction with methyl linoleate (53, 54). These differences in chemical selectivity would favor formation of dihydroperoxides with singlet oxygen. A second chemical selectivity difference is in the observed product distribution, when singlet oxygen reacts with methyl linoleate in solution, where 10- and 12-hydroperoxy linoleic methyl esters, in addition to the 9- and 13-hydroperoxy isomers, are generated (39, 55).

These authors suggested the potential of 10- and 12-hydroperoxy linoleate as biomarkers for  $^1\text{O}_2$  (55–57). These isomers may be intermediates for the formation of dihydroperoxides from  $^1\text{O}_2$ -mediated oxidation of CL.

Interestingly, characteristic fragment ions corresponding to 10- or 12-monohydroperoxides were not detected by MS/MS, suggesting that the second peroxidation occurred faster than the first peroxidation on the acyl chain. Alternatively, the dihydroperoxides may be generated by different mechanisms, such as incorporation of two oxygen molecules at the same time or involving rearrangement of 9- or 13-hydroperoxides to 10- or 12-hydroperoxides. In any case, the fact that the oxidized products of the linoleic acid side chains of CL, present in a liposome bilayer, are different from the oxidation products detected from methyl linoleate oxidation in solution suggests that the intramolecular interaction between the linoleic acyl chains may be an important contributor to oxidation mechanisms in the bilayer. It is still possible that 10- and 12-hydroperoxides may have lower ionization efficiencies or higher resistances to acyl chain cleavage.

In conclusion, we demonstrate by reverse-phase ion pair HPLC-MS/MS that  $^1\text{O}_2$  preferentially generates significant amounts of dihydroperoxides. Detection of CL dihydroperoxides species in biological systems may be the chemotype of  $^1\text{O}_2$ . 

The authors thank Professor Nancy Oleinick for sharing her equipment and technique to generate Pc 4-mediated  $^1\text{O}_2$ .

## REFERENCES

- Storz, P. 2006. Reactive oxygen species-mediated mitochondria-to-nucleus signaling: a key to aging and radical-caused diseases. *Sci. STKE*. **2006**: re3.
- Hoffmann, S., D. Spitkovsky, J. P. Radicella, B. Epe, and R. J. Wiesner. 2004. Reactive oxygen species derived from the mitochondrial respiratory chain are not responsible for the basal levels of oxidative base modifications observed in nuclear DNA of mammalian cells. *Free Radic. Biol. Med.* **36**: 765–773.
- Finkel, T., and N. J. Holbrook. 2000. Oxidants, oxidative stress and the biology of ageing. *Nature*. **408**: 239–247.
- Smith, M. A., C. A. Rottkamp, A. Nunomura, A. K. Raina, and G. Perry. 2000. Oxidative stress in Alzheimer's disease. *Biochim. Biophys. Acta*. **1502**: 139–144.
- Wallace, D. C. 2001. A mitochondrial paradigm for degenerative diseases and ageing. *Novartis Found. Symp.* **235**: 247–263.
- Toyokuni, S., K. Okamoto, J. Yodoi, and H. Hiai. 1995. Persistent oxidative stress in cancer. *FEBS Lett.* **358**: 1–3.
- Kowaltowski, A. J., N. C. de Souza-Pinto, R. F. Castilho, and A. E. Vercesi. 2009. Mitochondria and reactive oxygen species. *Free Radic. Biol. Med.* **47**: 333–343.
- Zimmerman, M. C., and I. H. Zucker. 2009. Mitochondrial dysfunction and mitochondrial-produced reactive oxygen species: new targets for neurogenic hypertension? *Hypertension*. **53**: 112–114.
- Marin-Garcia, J., Y. Pi, and M. J. Goldenthal. 2006. Mitochondrial-nuclear cross-talk in the aging and failing heart. *Cardiovasc. Drugs Ther.* **20**: 477–491.
- Fridovich, I. 1986. Biological effects of the superoxide radical. *Arch. Biochem. Biophys.* **247**: 1–11.
- Ramasarma, T. 1982. Generation of  $\text{H}_2\text{O}_2$  in biomembranes. *Biochim. Biophys. Acta*. **694**: 69–93.
- Girotti, A. W. 1998. Lipid hydroperoxide generation, turnover, and effector action in biological systems. *J. Lipid Res.* **39**: 1529–1542.
- Toufektsian, M. C., F. R. Boucher, S. Tanguy, S. Morel, and J. G. de Leiris. 2001. Cardiac toxicity of singlet oxygen: implication in reperfusion injury. *Antioxid. Redox Signal.* **3**: 63–69.
- Lee, J. W., H. Miyawaki, E. V. Bobst, J. D. Hester, M. Ashraf, and A. M. Bobst. 1999. Improved functional recovery of ischemic rat hearts due to singlet oxygen scavengers histidine and carnosine. *J. Mol. Cell. Cardiol.* **31**: 113–121.
- Grether-Beck, S., S. Olaizola-Horn, H. Schmitt, M. Grewe, A. Jahnke, J. P. Johnson, K. Briviba, H. Sies, and J. Krutmann. 1996. Activation of transcription factor AP-2 mediates UVA radiation- and singlet oxygen-induced expression of the human intercellular adhesion molecule 1 gene. *Proc. Natl. Acad. Sci. USA*. **93**: 14586–14591.
- Prado, F. M., M. C. Oliveira, S. Miyamoto, G. R. Martinez, M. H. Medeiros, G. E. Ronsein, and P. Di Mascio. 2009. Thymine hydroperoxide as a potential source of singlet molecular oxygen in DNA. *Free Radic. Biol. Med.* **47**: 401–409.
- Davies, M. J. 2003. Singlet oxygen-mediated damage to proteins and its consequences. *Biochem. Biophys. Res. Commun.* **305**: 761–770.
- Khan, A. U., and M. Kasha. 1994. Singlet molecular oxygen in the Haber-Weiss reaction. *Proc. Natl. Acad. Sci. USA*. **91**: 12365–12367.
- Nicholls, S. J., and S. L. Hazen. 2009. Myeloperoxidase, modified lipoproteins, and atherogenesis. *J. Lipid Res.* **50** (Suppl.): 346–351.
- Pitt, A. R., and C. M. Spickett. 2008. Mass spectrometric analysis of HOCl- and free-radical-induced damage to lipids and proteins. *Biochem. Soc. Trans.* **36**: 1077–1082.
- Nicholls, S. J., L. Zheng, and S. L. Hazen. 2005. Formation of dysfunctional high-density lipoprotein by myeloperoxidase. *Trends Cardiovasc. Med.* **15**: 212–219.
- Hoffmann, B., A. Stockl, M. Schlame, K. Beyer, and M. Klingenberg. 1994. The reconstituted ADP/ATP carrier activity has an absolute requirement for cardiolipin as shown in cysteine mutants. *J. Biol. Chem.* **269**: 1940–1944.
- Petrosillo, G., G. Casanova, M. Matera, F. M. Ruggiero, and G. Paradies. 2006. Interaction of peroxidized cardiolipin with rat-heart mitochondrial membranes: induction of permeability transition and cytochrome c release. *FEBS Lett.* **580**: 6311–6316.
- Ott, M., J. D. Robertson, V. Gogvadze, B. Zhivotovsky, and S. Orrenius. 2002. Cytochrome c release from mitochondria proceeds by a two-step process. *Proc. Natl. Acad. Sci. USA*. **99**: 1259–1263.
- Gonzalez, F., J. J. Bessoule, F. Rocchiccioli, S. Manon, and P. X. Petit. 2005. Role of cardiolipin on tBid and tBid/Bax synergistic effects on yeast mitochondria. *Cell Death Differ.* **12**: 659–667.
- Nukuna, B. N., G. Sun, and V. E. Anderson. 2004. Hydroxyl radical oxidation of cytochrome c by aerobic radiolysis. *Free Radic. Biol. Med.* **37**: 1203–1213.
- Kim, J., M. E. Rodriguez, M. Guo, M. E. Kenney, N. L. Oleinick, and V. E. Anderson. 2008. Oxidative modification of cytochrome c by singlet oxygen. *Free Radic. Biol. Med.* **44**: 1700–1711.
- Kim, J., M. E. Rodriguez, N. L. Oleinick, and V. E. Anderson. 2010. Photo-oxidation of cardiolipin and cytochrome c with bilayer-embedded Pc 4. *Free Radic. Biol. Med.* **49**: 718–725.
- He, J., H. E. Larkin, Y. S. Li, D. Richter, S. I. Zaidi, M. A. Rodgers, H. Mukhtar, M. E. Kenney, and N. L. Oleinick. 1997. The synthesis, photophysical and photobiological properties and in vitro structure-activity relationships of a set of silicon phthalocyanine PDT photosensitizers. *Photochem. Photobiol.* **65**: 581–586.
- Kim, J., H. Fujioka, N. L. Oleinick, and V. E. Anderson. 2010. Photosensitization of intact heart mitochondria by the phthalocyanine Pc 4: correlation of structural and functional deficits with cytochrome c release. *Free Radic. Biol. Med.* **49**: 726–732.
- Rodriguez, M. E., J. Kim, G. B. Delos Santos, K. Azizuddin, J. Berlin, V. E. Anderson, M. E. Kenney, and N. L. Oleinick. 2010. Binding to and photo-oxidation of cardiolipin by the phthalocyanine photosensitizer Pc 4. *J. Biomed. Opt.* **15**: 051604.
- Minkler, P. E., and C. L. Hoppel. 2010. Separation and characterization of cardiolipin molecular species by reverse-phase ion pair high-performance liquid chromatography-mass spectrometry. *J. Lipid Res.* **51**: 856–865.
- Ventrella, A., L. Catucci, G. Mascolo, A. Corcelli, and A. Agostiano. 2007. Isolation and characterization of lipids strictly associated to PSII complexes: focus on cardiolipin structural and functional role. *Biochim. Biophys. Acta*. **1768**: 1620–1627.
- Lesnefsky, E. J., M. S. Stoll, P. E. Minkler, and C. L. Hoppel. 2000. Separation and quantitation of phospholipids and lysophospholipids by high-performance liquid chromatography. *Anal. Biochem.* **285**: 246–254.

35. Hsu, F. F., J. Turk, E. R. Rhoades, D. G. Russell, Y. Shi, and E. A. Groisman. 2005. Structural characterization of cardiolipin by tandem quadrupole and multiple-stage quadrupole ion-trap mass spectrometry with electrospray ionization. *J. Am. Soc. Mass Spectrom.* **16**: 491–504.
36. Hager, J. W., and J. C. Yves Le Blanc. 2003. Product ion scanning using a Q-q-Q linear ion trap (Q TRAP) mass spectrometer. *Rapid Commun. Mass Spectrom.* **17**: 1056–1064.
37. Domingues, M. R., A. Reis, and P. Domingues. 2008. Mass spectrometry analysis of oxidized phospholipids. *Chem. Phys. Lipids.* **156**: 1–12.
38. Tyurin, V. A., Y. Y. Tyurina, M. Y. Jung, M. A. Tungekar, K. J. Wasserloos, H. Bayir, J. S. Greenberger, P. M. Kochanek, A. A. Shvedova, B. Pitt, et al. 2009. Mass-spectrometric analysis of hydroperoxy- and hydroxy-derivatives of cardiolipin and phosphatidylserine in cells and tissues induced by pro-apoptotic and pro-inflammatory stimuli. *J. Chromatogr. B Analyt. Technol. Biomed. Life Sci.* **877**: 2863–2872.
39. Zhang, W., M. Sun, and R. G. Salomon. 2006. Preparative singlet oxygenation of linoleate provides doubly allylic dihydroperoxides: putative intermediates in the generation of biologically active aldehydes in vivo. *J. Org. Chem.* **71**: 5607–5615.
40. Jemal, M., and Z. Ouyang. 2000. The need for chromatographic and mass resolution in liquid chromatography/tandem mass spectrometric methods used for quantitation of lactones and corresponding hydroxy acids in biological samples. *Rapid Commun. Mass Spectrom.* **14**: 1757–1765.
41. Kukreja, R. C., K. E. Loesser, A. A. Kearns, S. A. Naseem, and M. L. Hess. 1993. Protective effects of histidine during ischemia-reperfusion in isolated perfused rat hearts. *Am. J. Physiol.* **264**: H1370–H1381.
42. Kaplan, P., M. Matejovicova, P. Herijgers, and W. Flameng. 2005. Effect of free radical scavengers on myocardial function and Na<sup>+</sup>, K<sup>+</sup>-ATPase activity in stunned rabbit myocardium. *Scand. Cardiovasc. J.* **39**: 213–219.
43. Berneburg, M., S. Grether-Beck, V. Kurten, T. Ruzicka, K. Briviba, H. Sies, and J. Krutmann. 1999. Singlet oxygen mediates the UVA-induced generation of the photoaging-associated mitochondrial common deletion. *J. Biol. Chem.* **274**: 15345–15349.
44. Jiang, J., Z. Huang, Q. Zhao, W. Feng, N. A. Belikova, and V. E. Kagan. 2008. Interplay between bax, reactive oxygen species production, and cardiolipin oxidation during apoptosis. *Biochem. Biophys. Res. Commun.* **368**: 145–150.
45. Kagan, V. E., V. A. Tyurin, J. Jiang, Y. Y. Tyurina, V. B. Ritov, A. A. Amoscato, A. N. Osipov, N. A. Belikova, A. A. Kapralov, V. Kini, et al. 2005. Cytochrome *c* acts as a cardiolipin oxygenase required for release of proapoptotic factors. *Nat. Chem. Biol.* **1**: 223–232.
46. Pope, S., J. M. Land, and S. J. Heales. 2008. Oxidative stress and mitochondrial dysfunction in neurodegeneration; cardiolipin a critical target? *Biochim. Biophys. Acta.* **1777**: 794–799.
47. Petrosillo, G., N. Moro, F. M. Ruggiero, and G. Paradies. 2009. Melatonin inhibits cardiolipin peroxidation in mitochondria and prevents the mitochondrial permeability transition and cytochrome *c* release. *Free Radic. Biol. Med.* **47**: 969–974.
48. Perier, C., K. Tieu, C. Guegan, C. Caspersen, V. Jackson-Lewis, V. Carelli, A. Martinuzzi, M. Hirano, S. Przedborski, and M. Vila. 2005. Complex I deficiency primes Bax-dependent neuronal apoptosis through mitochondrial oxidative damage. *Proc. Natl. Acad. Sci. USA.* **102**: 19126–19131.
49. Lin, D., J. Zhang, and L. M. Sayre. 2007. Synthesis of six epoxy-ketooctadecenoic acid (EKODE) isomers, their generation from nonenzymatic oxidation of linoleic acid, and their reactivity with imidazole nucleophiles. *J. Org. Chem.* **72**: 9471–9480.
50. Sun, M., and R. G. Salomon. 2004. Oxidative fragmentation of hydroxy octadecadienoates generates biologically active gamma-hydroxyalkenals. *J. Am. Chem. Soc.* **126**: 5699–5708.
51. Roginskii, V. A. 1990. A kinetic model of peroxidation in a lipid bilayer. *Mol. Biol.* **24**: 1582–1589.
52. Roginsky, V. 2010. Oxidizability of cardiac cardiolipin in Triton X-100 micelles as determined by using a Clark electrode. *Chem. Phys. Lipids.* **163**: 127–130.
53. Monroe, B. M. 1981. Rate constants for the reaction of singlet oxygen with conjugated dienes. *J. Am. Chem. Soc.* **103**: 7253–7256.
54. Tanielian, C., and R. Mechlin. 1994. Reaction and quenching of singlet molecular oxygen with esters of polyunsaturated fatty acids. *Photochem. Photobiol.* **59**: 263–268.
55. Thomas, M. J., and W. A. Pryor. 1980. Singlet oxygen oxidation of methyl linoleate: isolation and characterization of the NaBH<sub>4</sub>-reduced products. *Lipids.* **15**: 544–548.
56. Sevanian, A., and P. Hochstein. 1985. Mechanisms and consequences of lipid peroxidation in biological systems. *Annu. Rev. Nutr.* **5**: 365–390.
57. Orfanopoulos, M., and C. S. Foote. 1987. The ene reaction of singlet oxygen with olefins. *Free Radic. Res. Commun.* **2**: 321–326.